a decrease in the negative change in binding enthalpy ($\Delta\Delta H$; 6.9 kJ mol^{-1}) accompanied by a small decrease in the binding constant (K_a; 1.78×10^8 mol^{-1}). These thermodynamic changes might originate from the removal of a hydrogen bond between the Nδ2 atom of L-Asn31 and the O atom of HEL-His15 and from the conversion of a hydrogen bond between the Oδ1 atom of L-Asn31 and the Nζ atom of HEL-Lys96 to a salt bridge. The hydrogen bond present in the wild-type Fv–HEL complex, but absent from the LN31D–HEL complex, is expected to be weak because the distance between the two atoms involved in this bond are close to the limit for hydrogen bonding to occur. Therefore, the contribution of this hydrogen bond to the strength of the antibody-antigen interaction is most likely to be relatively small compared to other bonds. On the contrary, the hydrogen bond that was converted to a salt bridge in the mutant Fv was found by free energy simulations to be highly polarized (72). Thus, the effect of deleting this hydrogen bond is expected to be greater than the former. Furthermore, the changes in thermodynamic parameters of the antibody-antigen interaction are most likely caused by the substitution of a hydrogen bond with a salt bridge. The free energy simulations described above (72); however, suggest that the substitution of a hydrogen bond with a salt bridge between L-Asn31Asp and HEL-Lys96 or between L-Asn31Glu and HEL-Lys96 is expected to stabilize the interaction between HyHEL-10 and HEL. This indicates a discrepancy between the predicted result (calculated data) and our present experimental data, which shows that the substitution destabilizes the interaction ($\Delta\Delta G$, 3.8 kJ mol^{-1}). However, our data is supported by a previous study showing that the substitutions of L-Asn31 with Asp and with Glu using the single-chain variable fragment of the HyHEL-10 mutant antibodies, LN31D scFv and LN31E scFv, stabilize the interaction between the mutant antibodies and HEL [$\Delta\Delta G = 1.4 \pm 0.3$ kcal mol^{-1} (5.9 ± 1.3 kJ mol^{-1}) and $\Delta\Delta G = 5.7 \pm 0.1$ kcal mol^{-1} (23.8 ± 0.4 kJ mol^{-1}), respectively] (49). These thermodynamic parameters might indicate that the charged antigen epitope residues with a positive charge, corresponding to Lys96 of HEL in this case, are more stable by coupling with the donor and/or acceptor of the hydrogen bond in the neutral state, corresponding to the side chain of L-Asn31 in this case, than by coupling with its counterpart charge, corresponding to the side chain of L-Asp31 with a negative charge in this case (49). Furthermore, analysis of charged amino acid side chains (Arg, Lys, Glu, and Asp) buried at the intermolecular interfaces indicates that oriented dipoles are usually preferred over countercharges in stabilizing these buried residues (69).

Thermodynamics analysis of the interaction between LN31A and HEL, suggests that the Ala substitution at L-Asn31 leads to a drastic decrease in binding enthalpy ($\Delta\Delta H$; 50.8 kJ mol^{-1}), which cannot be compensated for by the large decrease in entropic loss ($T\ \Delta\Delta S$; 34.5 kJ mol^{-1}), thus resulting in a decrease in Gibbs energy ($\Delta\Delta G$; 16.3 kJ mol^{-1}). It has been suggested that a large negative change in enthalpy mostly originates from the formation of hydrogen bond and/or van der Waals interactions during binding (32, 33, 43, 55). Thus, it is conceivable that in the LN31A–HEL interaction, the substitution of Asn with Ala might introduce an interfacial structure different from that in the wild-type

Fv–HEL complex as well as many changes in the interfacial non-covalent bonds between the antibody and antigen, including loss of van der Waals interactions and hydrogen bonds with large energetic contributions to binding in the wild-type Fv–HEL complex. The binding constant of the LN31A–HEL interaction is much lower than that of the wild-type interaction by about 3 orders of magnitude, despite the large decrease in entropic loss that results partly from a reduction in the conformational flexibility of the antibody upon complexation (73, 74) (Table 1). Unexpectedly, the binding constant is lower for the LN31A–HEL interaction than for the HY33A–HEL interaction, in which the mutation site (H-Tyr33) is considered as a hot spot of the paratope in the HyHEL-10 Fv–HEL interaction (55). These findings suggest that the hydrogen bond between the Oδ1 atom of L-Asn31 and the Nζ atom of HEL-Lys96, and/or the deleted van der Waals contacts between atoms on the side chain of L-Asn31 (Oδ1, Nδ2 and Cγ atoms) and HEL might confer an entropy disadvantage, but it confers an enthalpy advantage and thus plays a crucial role in the affinity between the wild-type antibody and the HEL target. Thus, we conclude that L-Asn31 is one of the energetic hot spots (75) in the HyHEL-10 Fv–HEL interaction.

L-Asn32: critical contribution of Nδ2 in stabilizing the complex through hydrogen bond formation— The crystal structure of the LN32D–HEL complex has many changes in structural features, when compared to the wild-type Fv–HEL complex including a large difference in the orientation of HEL to VL and/or VH (Table 2), a decrease in the antigen-antibody interfacial area (Supplemental Table S3), conformational changes in local structure at, near, and far from the mutation site, movement of interfacial water molecules accompanied by rearrangements of the hydrogen bonding network, as well as many changes (loss and/or gain) in the antigen-antibody interaction resulting from these structural changes (Fig. 4B, Fig 5A, Supplemental Table S2, and S4). These structural differences between the LN32D–HEL and wild-type Fv–HEL complexes are similar to the differences between the LN92D–HEL and wild-type Fv–HEL complexes apart from the loss of the hydrogen bond between the Nδ2 atom of L-Asn32 and the O atom of HEL-Gly16 that resulted from the substitution of Asn with Asp in LN32D. This hydrogen bond is unexpectedly conserved in the LN92D–HEL complex, whereas all the other changes described above are similar to those in the LN32D–HEL complex. By comparison, the loss of the hydrogen bond between the Nδ2 atom of L-Asn92 and the O atom of HEL-Asn19 observed in the LN92D–HEL complex because of the substitution of Asn with Asp in LN92D, is not conserved in the LN32D–HEL complex, despite the lack of mutation at L-Asn92 in LN32D (Fig 5A, Supplemental Table S4). Taken together, these observations suggest that the formation of the hydrogen bond between the Nδ2 atom of L-Asn32 and the O atom of HEL-Gly16 induces the formation of other interactions, including the hydrogen bond between the Nδ2 atom of L-Asn92 and the O atom of HEL-Asn19. The number of non-covalent bonds between antibody and antigen was higher for the LN32D–HEL interaction, than for the wild-type Fv–HEL interaction with higher affinity (Supplemental Table S5). The LN32D–HEL interaction had a lower binding constant than the wild-type Fv–HEL

interaction by 2 orders of magnitude (Table 1). Therefore, even if large conformational changes are introduced by the other interfacial residues on CDRs and form other interactions, these newly formed interactions cannot compensate for the energetic loss of the hydrogen bond between the Nδ2 atom of L-Asn32 and the O atom of HEL-Gly16.

At the interface of HyHEL-10 Fv–HEL, about 20 direct hydrogen bonds have been observed between the antigen and the antibody (45, 55) (Supplemental Table S4). For example, H-Ser52, H-Ser54, and H-Ser56 also contact the antigen by forming hydrogen bonds via their side-chain hydroxyl group. Thermodynamic analysis of the interaction between the Fv mutants HS52A, HS54A, and HS56A and HEL show that the small decrease in the favorable enthalpy change and in the unfavorable entropy change, results in a slight increase in the value of the binding constant (Supplemental Table S6) (Yokota, unpublished data). This result suggests that the hydrogen bonds, which have been deleted in the mutant antibody-antigen interactions, have an energetically unfavorable entropy effect in the antigen-antibody interaction, rather than supplemental minor contribution to the interaction. Taken together, these results suggest that the energetic contribution of hydrogen bonds to the antigen-antibody interaction varies enormously and ranges from strong to weak in terms of affinity. Our results suggest that the more buried the hydrogen bond is at the interface, the greater its energetic contribution. L-Asn32 in the wild-type Fv–HEL complex is completely buried at the interface and has an accessible surface area (ASA) of 0 $Å^2$. By comparison, H-Ser54 and H-Ser56 are relatively exposed with ASAs of 60 $Å^2$ and 25 $Å^2$, respectively. Several other reports support our notion that the more buried the hydrogen bond is at the interface, the stronger the bond. Strong hydrogen bonds buried at the interface are observed in the interaction between thermolysin and its inhibitor (28) and between hemagglutinin (HA) of a mutant influenza virus and its monoclonal antibody (76). In the interaction between the D1.3 antibody, which is the anti-HEL antibody as same as HyHEL-10, and the anti-D1 antibody E5.2, the binding energy of the strongest hydrogen bond among those buried at the interface is 4.3 kcal mol^{-1}, whereas the binding energies of exposed hydrogen bonds are only 1.3–1.7 kcal mol^{-1} (77). The hydrogen bond between the Nδ2 atom of L-Asn32 and the O atom of HEL-Gly16 might make the interface rigid with its high energy and result in an unfavorable entropy effect in the interaction. However, this type of hydrogen bond might be considered to have a greater favorable enthalpy effect than an unfavorable entropy effect, and thus make an important contribution to the acquirement of affinity for the antigen. We can conclude that this type of hydrogen bond is one of the most critical in the interaction, and thus cannot be compensated for by other conformational changes or by formatting other non-covalent bonds.

In the interaction between L-Asn32A and HEL, the substitution of Asn with Ala at L-32 leads to a large decrease in binding enthalpy ($\Delta\Delta H$; 25.7 kJ mol^{-1}), exceeding the decrease in entropic loss ($T\Delta\Delta S$; 10.1 kJ mol^{-1}), resulting in a great loss in Gibbs energy ($\Delta\Delta G$; 15.6 kJ mol^{-1}). Thermodynamic parameters suggest that this mutation introduces changes to the interfacial structure and non-covalent bonds found in wild-type–HEL, including loss of van der

Waals interactions and hydrogen bonds with large energetic contributions to the Fv–HEL interaction, which are also seen in LN31A–HEL and LN32D–HEL interactions. In each case, the Asn to Ala substitution decreased the affinity of the antibody for the antigen, suggesting that the Asn residue at L-32 contributes to generating affinity and specificity of the HyHEL-10 Fv–HEL interaction as one of the "hot spot" residues in the interaction.

L-Asn92: a small enthalpic gain results in minor contribution to affinity— As already described, the structural differences between the LN92D–HEL and the wild-type Fv–HEL complex (Table 2, Fig. 4B, Fig 5A, Supplemental Table S2, S3, S4, and S5) are similar to the differences between LN32D–HEL and the wild-type Fv–HEL complex. However, the thermodynamics parameters for LN92D–HEL are markedly different from those for LN32D–HEL. The substitution of Asn with Asp at the L-92 leads to a small decrease in binding enthalpy and no change in entropic loss, resulting in only a decrease in binding constant compared to the wild-type Fv–HEL interaction, whereas the substitution of Asn with Asp at L-32 leads to a drastic decrease in the binding enthalpy as well as a decrease in the binding constant. These results suggest that the difference in thermodynamic parameters between LN92D–HEL and LN32D–HEL interactions can be attributed to the presence and absence, respectively, of the hydrogen bond between the Nδ2 atom of L-Asn32 and the O atom of HEL-Gly16, and that the LN92D mutant maintains affinity for HEL because this hydrogen bond is maintained. It can be concluded that the hydrogen bond between the Nδ2 atom of L-Asn92 and the O atom of HEL-Asn19 abolished by the substitution of Asn with Asp at L-92, like that at L-31 for LN31D, has only an incremental enthalpic contribution to the interaction the loss of which can be compensated by changes in interfacial structure and/or formations of other non-covalent bonds.

Insight into the role of Asn residues in antigen-antibody interactions— Our findings can be summarized as follows: 1) Isothermal titration calorimetric analysis shows that all mutations involving Asn residues lead to a decrease in the negative enthalpy change as well as a decrease in the association constants of the interaction. 2) The contribution of two hydrogen bonds is small, the deletion of which leads to only a slight decrease in affinity of the antibody for the antigen. By comparison, two hydrogen bonds show enthalpic gain, despite entropic loss perhaps due to stiffening of the interface by the bonds, and play a major role in the antigen-antibody interaction and thus in the affinity of the antibody for the antigen. 3) Structural analyses revealed that the effects of mutations involving Asn residues on the structure of the antigen-antibody complexes were compensated for by conformational changes and/or by gains of other interactions. 4) Hydrogen bonding buried at the interfacial area, such as those of L-Asn32, have an enthalpic advantage over those exposed at the interfacial area, and thus contribute significantly to the affinity of the antibody for the antigen; the deletion of these hydrogen bonds cannot be compensated for by structural changes. These results suggest that the contribution of Asn residues to the antigen-antibody interaction depends on the structure of the local interfacial area, which is independent of their potential for hydrogen bond formation. Formation of a salt bridge between the side chains of Asp (and/or Glu)

and Arg (and/or Lys) residues at the complex interface often contributes to the affinity and specificity of an interaction (78-80). Asp is used at a higher than the expected frequency in CDRs (5, 11, 80). It has been reported that in the interaction between HyHEL-5 and HEL, the loss of a salt bridge at the interface causes a remarkable decrease in the binding constant (79). By comparison, some Asp residues make only a minor contribution to the affinity of the protein interaction through salt bridges that originate from enthalpy-entropy compensation arising from the introduction of interfacial water molecules (44). Lines of evidence from previous reports suggest that the contribution of charged residues to the strength of protein interactions also depends on interfacial structure.

Based on our structural and thermodynamics analysis on mutations involving Asn residues described above, we will discuss why Asn residues are a preferred amino acid for stabilizing antigen-antibody complexes. First, the side chain of Asn makes less van der Waals contacts with the target antigen and has less of a tendency to form a hydrophobic environment than that of Trp and Tyr, which is the most common residue in CDRs (55). By comparison, Asn has the ability to make more contacts and more types of contacts than does Gly, Ala or Ser. Second, the steric hindrance attributed to Asn because of its moderate size compared to other residues, is low enough to reduce the loss in conformational entropy in the antigen-antibody interaction. Support for this notion comes from the report that Asn is used in antigen-antibody interactions at a higher frequency than Gln, which has similar properties to Asn but generates more steric hindrance because of its larger size (80, 81). Third, and most importantly, the side chain of Asn has a neutral and polar amide group consisting of the donor and acceptor of hydrogen bonding atoms Oδ1 and Nδ2 under neutral pH conditions. This functional group confers the ability for Asn to accommodate both positive and negative charges of the antigen and to form many hydrogen bond interactions with its target at the interface of the antibody. Thus, Asn can provide this functional group consisting of two atoms of Oδ1 and Nδ2 for strong hydrogen bond formation, and their contribution to the antigen-antibody interaction can be attributed to their limited flexibility and accessibility at the complex interface. Tsumoto *et al.* (43) and Shiroishi *et al.* (55) have shown that Tyr residues, the most common in CDRs, are energetic hot-spot at some sites but can also provide only a minor contribution to the antigen-antibody interaction, and that these properties of Tyr depend on the local structure. For specific antigen recognition, such properties might be critical for the preparation of binding sites, and therefore, Asn might be an appropriate residue for antigen recognition through hydrogen bond formation by using this functional group. Finally, it should be noted that Asn residues rarely appear at conserved positions in frameworks of VL, despite their high frequent appearance in CDRs (Supplemental Fig. S1). This fact also might support that Asn is an amino acid specifically used for binding to an antigen and for stabilizing the antigen–antibody complexes.

Acknowledgments— We thank N. Sakabe, S. Wakatsuki, M. Suzuki, and N. Igarashi at the Photon Factory for their kind help with data collection.

REFERENCES

1. Böhm, H.-J. and Schneider, G. (2003). *Protein-Ligand Interactions: From Molecular Recognition to Drug Design*, Methods and Principles in Medicinal Chemistry **19**,Wiley-VCH, Weinheim
2. Kabat, E. A., Wu, T. T., and Bilofsky, H. (1976) *Proc. Natl. Acad. Sci. U. S. A.* **73**, 4471-4473
3. Kabat, E A, ,Wu, T.T, and Bilofsky, H. (1977) *J. Biol. Chem.* **252**, 6609-6616
4. Padlan, E. A. (1990) *Proteins Struct.Funct. Genet.* **7**, 112-124
5. Mian, I. S., Bradwell, A. R., and Olson, A. J. (1991) *J. Mol. Biol.* **217**, 133-151
6. Sheriff, S., Silverton, E. W., Padlan, E. A., Cohen, G. H., Smith-Gill, S. J., Finzel, B. C., and Davies, D. R. (1987) *Proc. Natl. Acad. Sci. U. S. A,* **84**, 8075-8079
7. Chothia, C. and Lesk, A. M. (1987) *J. Mol. Biol.*, **196**, 901-917
8. Padlan, E. A., Silverton, E. W., Sheriff, S., Cohen, G. H., Smith-Gill, S. J., and Davies, D. R. (1989) *Proc. Natl. Acad. Sci. U. S. A.*, **86**, 5938-5942
9. Wilkinson RA, Piscitelli C, Teintze M, Cavacini LA, Posner MR, Lawrence CM. (2005) *J. Virol.* **79**, 13060-13069
10. Chothia, C. and Lesk, A. M. (1987) *J. Mol. Biol.*, **196**, 901-917
11. Jackson, R. M. (1999) *Protein Sci.*, **8**, 603-613
12. Clements, C. S., Dunstone, M. A., Macdonald, W. A., McCluskey, J., and Rossjohn, J. (2006) *Curr. Opin. Struct. Biol.* **16**, 787-795
13. Wang, Y., Shen, B. J., and Sebald, W. (1997) *Proc. Natl. Acad. Sci. U. S. A.* **94**, 1657-1662
14. Brautigam, C. A., and Steitz, T. A. (1998) *Curr. Opin. Struct. Biol.* **8**, 54-63
15. Chothia, C., Lesk, A. M., Tramontano, A., Levitt, M., Smith-Gill, S. J., Air, G., Sheriff, S., Padlan, E. A., Davies, D., Tulip, W. R., and Colman, P. M., Spinelli, S., Alzari, P. M., and Poljak, R. J. (1989) *Nature* **342**, 877-883
16. Davies, D. R., Padlan, E. A., and Sheriff, S. (1990) *Annu. Rev. Biochem.* **59**, 439-473
17. Janin, J., and Chothia, C. (1990) *J. Biol. Chem.* **265**, 16027-16030
18. Smith-Gill, S. J. (1991) *Curr. Opin. Biotechnol.* **2**, 568-575
19. Mariuzza, R. A., and Poljak, R. J. (1993) *Curr. Opin. Immunol.* **5**, 50-55
20. Fischer, E. (1894) *Ber. Dtsch. Chem. Ges.* **27**, 2984–2993
21. Koshland, D.E. (1958) *Proc. Natl. Acad. Sci. U.S.A* . **44**, 98–104
22. Lo Conte, L., Chothia, C., and Janin, J. (1999) *J. Mol. Biol.* **285**, 2177-2198
23. Jones, S., and Thornton, J. M. (1996) *Proc. Natl. Acad. Sci. U. S. A.* **93**, 13-20
24. Chothia, C., and Janin, J. (1975) *Nature* **256**, 705-708
25. Desiraju, G. R., and Steiner, T. (2001) *The Weak Hydrogen Bond: In Structural Chemistry and Biology.* International Union of Crystallography Monographs on Crystallography, 9, Oxford Univ Press, Oxford
26. Fersht, A. R., Shi, J. P., Knill-Jones, J., Lowe, D. M., Wilkinson, A. J., Blow, D. M., Brick, P., Carter, P., Waye, M. M., and Winter, G. (1985) *Nature* **314**, 235-238

27. Bartlett, P. A., and Marlowe, C. K. (1987) *Science* **235**, 569-571
28. Tronrud, D. E., Holden, H. M., and Matthews, B. W. (1987) *Science* **235**, 571-574
29. Mandel-Gutfreund, Y., Schueler, O., and Margalit, H. (1995) *J. Mol. Biol.* **253**, 370-382
30. Fields, B. A., Goldbaum, F. A., Dall'Acqua, W., Malchiodi, E. L., Cauerhff, A., Schwarz, F. P., Ysern, X., Poljak, R. J., and Mariuzza, R. A. (1996) *Biochemistry* **35**, 15494-15503
31. James, L. C., and Tawfik, D. S. (2003) *Protein Sci.* **12**, 2183-2193
32. Torigoe, H., Nakayama, T., Imazato, M., Shimada, I., Arata, Y., and Sarai, A. (1995). *J. Biol. Chem.* **270**, 22218-22222
33. Connelly, P. R., Aldape, R. A., Bruzzese, F. J., Chambers, S. P., Fitzgibbon, M. J., Fleming, M. A., Itoh, S., Livingston, D. J., Navia, M. A., Thomson, J. A., and Wilson, K. P. (1994) *Proc. Natl. Acad. Sci. U. S. A.* **91**, 1964-1968
34. Bhat, T. N., Bentley, G. A., Boulot, G., Greene, M. I., Tello, D., Dall'Acqua, W., Souchon, H., Schwarz, F. P., Mariuzza, R. A., and& Poljak, R. J. (1994) *Proc. Natl. Acad. Sci. U. S. A.* **91**, 1089-1093
35. Webster, D. M., Henry, A. H., and Rees, A. R. (1994) *Curr. Opin. Struct. Biol.* 4, 123-129
36. Davies, D. R., and Cohen, G. H. (1996) *Proc. Natl. Acad. Sci. U. S. A.* **93**, 7-12
37. Colman, P. M. (1988) *Adv. Immunol.* 43, 99-132
38. Braden, B. C., and Poljak, R. J. (1995) *Faseb J.* **9**, 9-16
39. Padlan, E. A. (1996) *Adv. Protein. Chem.* **49**, 57-133
40. Brummell, D. A., Sharma, V. P., Anand,N.N., Bilous,D., Dubuc, G., Michniewicz, J., MacKenzie, C. R., Sadowska, J., Sigurskjold, B. W., Sinnott, B., Young, N. M., Bundle, D. R., and Narang, S. A. (1993) *Biochemistry* **32**, 1180-1187
41. Sundberg, E. J., Urrutia, M., Braden, B. C., Isern, J., Tsuchiya, D., Fields, B. A., Malchiodi, E. L., Tormo, J., Schwarz, F. P., and Mariuzza, R. A. (2000) *Biochemistry* **39**, 15375-15387
42. Tsumoto, K., Ueda, Y., Maenaka, K., Watanabe, K., Ogasahara, K., Yutani, K., and Kumagai, I. (1994) *J. Biol. Chem.* **269**, 28777-28782
43. Tsumoto, K., Ogasahara, K., Ueda, Y., Watanabe, K., Yutani, K., and Kumagai, I. (1995) *J. Biol. Chem.* **270**, 18551-18557
44. Tsumoto, K., Ogasahara, K., Ueda, Y., Watanabe, K., Yutani, K., and Kumagai, I. (1996) *J. Biol. Chem.* **271**, 32612-32616
45. Kondo, H., Shiroishi, M., Matsushima, M., Tsumoto, K., and Kumagai, I. (1999) *J. Biol. Chem.* **274**, 27623-27631
46. Nishimiya, Y., Tsumoto, K., Shiroishi, M., Yutani, K., and Kumagai, I. (2000) *J. Biol. Chem.* **275**, 12813-12820
47. Shiroishi, M., Yokota, A., Tsumoto, K., Kondo, H., Nishimiya, Y., Horii, K., Matsushima, M., Ogasahara, K., Yutani, K., and Kumagai, I. (2001) *J. Biol. Chem.* **276**, 23042-23050
48. Yokota, A., Tsumoto, K., Shiroishi, M., Kondo, H., and Kumagai, I. (2003) *J. Biol.*

Chem. **278**, 5410-5418
49. Pons, J., Rajpal, A., and Kirsch, J. F. (1999) *Protein Sci.* 8, 958-968
50. Rajpal, A., Taylor, M. G., and Kirsch, J. F. (1998) *Protein Sci.* **7**, 1868-1874
51. Ueda, Y., Tsumoto, K., Watanabe, K., and Kumagai, I. (1993) *Gene* **129**, 129-134
52. Tsumoto, K., Nakaoki, Y., Ueda, Y., Ogasahara, K., Yutani, K., Watanabe, K., and Kumagai, I. (1994) *Biochem. Biophys. Res. Commun.* **201**, 546-551
53. Merk, H., Stiege, W., Tsumoto, K., Kumagai, I., and Erdmann, V. A. (1999) *J. Biochem.* **125**, 328-333
54. Ueda, H., Tsumoto, K., Kubota, K., Suzuki, E., Nagamune, T., Nishimura, H., Schueler, P. A., Winter, G., Kumagai, I., and Mohoney, W. C. (1996) *Nat. Biotechnol.* **14**, 1714-1718
55. Shiroishi, M., Tsumoto, K., Tanaka, Y., Yokota, A., Nakanishi, T., Kondo, H., and Kumagai, I. (2007) *J. Biol. Chem.* **282**, 6783-6791
56. Kunkel, T. A., Roberts, J. D., and Zakour, R. A. (1987) *Methods Enzymol.* **154**, 367-382
57. Laemmli, U. K. (1970) *Nature* **227**, 680-685
58. Imoto, T., Johnson, T. M., North, A. C. T., Phillips, D. C., and Rupley, J. A. (1972) *Enzymes* **7**, 665-868
59. Leslie, A. G. W. (1992). *Joint CCP4 + ESF-EAMCB Newsletter on Protein Crystallography*. Protein Crystallography, p.26, Warrington, UK
60. Evans, P. R. (1993). *Proceedings of CCP4 Study Weekend*, pp. 114-122, Warrington, UK.
61. French, S., and Wilson, K. (1978) *Acta Crystallogr. Sect. A* **34**, 517-525
62. Collaborative Computational Project (1994) *Acta Crystallogr. D* **50**, 760-763
63. Brunger, A. T., Adams, P. D., Clore, G. M., DeLano, W. L., Gros, P., Grosse-Kunstleve, R. W., Jiang, J. S., Kuszewski, J., Nilges, M., Pannu, N. S., Read, R. J., Rice, L. M., Simonson, T., and& Warren, G. L. (1998) *Acta Crystallogr. D* **54**, 905-921
64. Jones, T. A., Zou, J. Y., Cowan, S. W., and Kjeldgaard, M. (1991) *Acta Crystallogr A* **47** (Pt 2), 110-119
65. Kabsch, W. (1976) *Acta Crystallogr. Sect. A* **32**, 922-923
66. Kauzmann, W. (1959) *Adv. Protein Chem.* **14**, 1-63
67. Livingstone, J. R., Spolar, R. S., and Record, M. T., Jr. (1991) *Biochemistry* **30**, 4237-4244
68. Spolar, R. S., and Record, M. T., Jr. (1994) *Science* **263**, 777-784
69. Chothia, C. (1974) *Nature* **248**, 338-339
70. Ladbury, J. E., Wright, J. G., Sturtevant, J. M., and Sigler, P. B. (1994) *J. Mol. Biol.* **238**, 669-681
71. Myszka, D. G., Sweet, R. W., Hensley, P., Brigham-Burke, M., Kwong, P. D., Hendrickson, W. A., Wyatt, R., Sodroski, J., and Doyle, M. L. (2000) *Proc. Natl. Acad. Sci. U. S. A.* **97**, 9026-9031
72. Pomes, R., Willson, R. C., and McCammon, J. A. (1995) *Protein Eng.* **8**, 663-675
73. Willcox, B. E., Gao, G. F., Wyer, J. R., Ladbury, J. E., Bell, J. I., Jakobsen, B. K., and

van der Merwe, P. A. (1999) *Immunity* **10**, 357-365
74. Murphy, K. P., Freire, E., and Paterson, Y. (1995) *Proteins* **21**, 83-90
75. Clackson, T., and Wells, J. A. (1995) *Science* **267**, 383-386
76. Fleury, D., Wharton, S. A., Skehel, J. J., Knossow, M., and Bizebard, T. (1998) *Nat. Struct. Biol.* **5**, 119-123
77. Goldman, E. R., Dall'Acqua, W., Braden, B. C., and Mariuzza, R. A. (1997) *Biochemistry* **36**, 49-56
78. Aitio O, Hellman M, Kesti T, Kleino I, Samuilova O, Pääkkönen K, Tossavainen H, Saksela K, Permi P. (2008) *J. Mol. Biol.* **382**, 167-178
79. Wibbenmeyer, J. A., Schuck, P., Smith-Gill, S. J., and Willson, R. C. (1999) *J. Biol. Chem* .**274**, 26838-26842
80. Bogan, A. A., and Thorn, K. S. (1998) *J. Mol. Biol.* **280**, 1-9
81. Lee, K. H., Xie, D., Freire, E., and Amzel, L. M. (1994) *Proteins* **20**, 68-84

FOOTNOTES

The atomic coordinates and structure factors (codes 3A67, 3A6B, *and* 3A6C*) have been deposited in the Protein Data Bank, Research Collaboratory for Structural Bioinformatics, Rutgers University, New Brunswick, NJ (http://www.rcsb.org/).*

This work was supported by grants-in-aid for general research (to K. T. and I. K.).

The abbreviations used are: CDR, complementarity-determining region; HEL, hen egg white lysozyme; VH, variable region of immunoglobulin heavy chain; VL, variable region of immunoglobulin light chain; Fv, fragment of immunoglobulin variable regions; Fab, antigen-binding fragment of immunoglobulin; ITC, isothermal titration calorimetry; r.m.s.d., root-mean-square deviation.

The abbreviation used for mutants is, for example, LN31A, which is the mutant of HyHEL-10 Fv in which Ala is substituted for Asn-31 in the VL chain.

FIGURE LEGENDS

Fig. 1. The interaction between HyHEL-10 Fv and HEL.
A Overall structure of the wild-type HyHEL-10 Fv–HEL complex. The C-α schematic diagram of VL, VH, and HEL are shown in *green, cyan*, and *pink*, respectively. The residues investigated in this paper are shown in orange. Interfacial water molecules bridging Fv and HEL are represented by red balls.
B and ***C*** Local structure around the target sites investigated in this report. Interfacial Asn residues at site 31, 32 (***B***), and 92 (***C***) in the VL participating in the antigen-antibody interaction generated by the formation of direct hydrogen bonds with the antigen. The contacting residues in VL and HEL are shown by *green* and *pink* sticks, respectively. Direct hydrogen bonds and

indirect hydrogen bonds (via interfacial water molecules) between the antigen and antibody are indicated by red dashed lines. The figures were generated with WebLab Viewer (Molecular Simulations Inc., San Diego, CA, USA).

Fig. 2. Inhibition of lysozyme enzymatic activity by HyHEL-10 Fv
Experimental conditions are provided in the text. Symbols used: *solid squares* (–■–), wild type; *open circles* (–○–), LN31A; *solid circles* (–●–), LN31D; *open triangles* (–Δ–), LN32A; *solid triangles* (–▲–), LN32D; *solid crosses* (–×–), LN92D.

Fig. 3. Thermodynamic analyses of interactions between HyHEL-10 Fv mutants and HEL by isothermal titration calorimetry.
Thermogram and titration curves for LN31A–HEL (***A***), LN32D–HEL (***B***), and LN92D–HEL (***C***). The baseline obtained by titrating each mutant Fv solution (50 μM) with buffer was subtracted from the thermogram obtained by titrating the corresponding Fv solution with the HEL solution (5 μM).

Fig. 4. Comparison of local structures at the mutation site between mutant Fv–HEL and wild-type Fv–HEL complexes.
A, LN31D–HEL; ***B***, LN32D–HEL; ***C***, LN92D–HEL. C-α atoms of all polypeptide chains of each mutant complex are superimposed on those of the wild-type complex. Wild-type complex is shown in *gray*. Residues of VL, VH, and HEL in the mutant Fv–HEL complexes are shown in *green, cyan,* and *pink*, respectively. The positions marked "W" correspond to the water molecules (parentheses indicate wild-type water molecules) shown as red balls. Hydrogen bonds in the mutant Fv–HEL complexes and wild-type complex are depicted as red dotted lines and gray dotted lines, respectively. Salt bridges in the mutant complexes are depicted as blue broken lines. The hydrogen bonding (observed in the wild-type Fv–HEL complex) that is abolished in each mutation is represented as a gray thick dashed line.

Fig. 5. Comparison of local structures at sites other than the mutation site between mutant Fv–HEL and wild-type Fv–HEL complexes.
Local structures around L-Asn92 in the LN32D–HEL complex (***A***) and around L-Asn32 in the LN92D–HEL complex (***B***). Hydrogen bonds conserved in mutant and wild-type Fv–HEL complexes are omitted to facilitate visualization. Refer to Figure 4 for details.

Table 1 Thermodynamic parameters of mutant Fv–HEL interactions at 30°C and pH 7.2 in phosphate buffer.

Experimental protocols are described in the text. Data represent the average of at least three independent measurements. Errors for all values were within 5% for several experiments. The abbreviations used are as follows: n, stoichiometry; K_a, binding constant; ND, not determined; ΔG, ΔH, ΔS, and ΔC_p, changes in Gibbs energy, binding enthalpy, entropy, and heat capacity, respectively.

Mutant	n	K_a [$\times 10^7$ M^{-1}]	ΔG [kJ mol^{-1}]	$\Delta\Delta G$	ΔH [kJ mol^{-1}]	$\Delta\Delta H$	$T\Delta S$ [kJ mol^{-1}]	$T\Delta\Delta S$	ΔS [kJ mol^{-1} K^{-1}]	$\Delta\Delta S$	ΔC_p[a] [kJ mol^{-1} K^{-1}]	$\Delta\Delta C_p$[a]
Wild type	1.05	82.1	−51.7	0	−99.7	0	−48.0	0	−0.158	0	−1.53	0
LN31A	0.96	0.13	−35.4	16.3	−48.9	50.8	−13.5	34.5	−0.045	0.113	−2.35	−0.82
LN31D	0.94	17.8	−47.9	3.8	−92.8	6.9	−44.9	3.1	−0.148	0.01	−1.70	−0.17
LN32A	0.84	0.17	−36.1	15.6	−74.0	25.7	−37.9	10.1	−0.125	0.033	N.D.[b]	N.D.[b]
LN32D	0.97	0.93	−40.3	11.4	−47.2	52.5	−6.9	41.1	−0.023	0.135	−1.01	0.52
LN92D	0.85	14.0	−47.2	4.5	−94.6	5.1	−47.4	0.6	−0.156	0.002	-−1.68	−0.15

[a] The changes in heat capacity were calculated by performing measurements at four different temperatures, 25°C , 30°C, 35°C and 40°C, except for LN32A.

[b] The measurement for the association between the LN32A and HEL was performed only at one temperature (30°C), because the expressed and purified amount of LN32A mutant protein was too small for further analyses.

Table 2 RMSD in the C-α atoms of each chain (Å)

RMSD were obtained by superposing the C-α atom coordinates of each polypeptide chain (VL, VH, or HEL), the Fv portion (VL and VH), or all chains on the corresponding chain of the wild-type complex. RMSD were calculated with LSQKAB and COMPAR in the CCP4 suite. WT indicates wild type.

Complex		VL fit	VH fit	HEL fit	Fv fit	All fit
LN31D *vs* WT	VL	0.08	0.13	0.14	0.09	0.11
	VH	0.15	0.08	0.10	0.09	0.09
	HEL	0.25	0.13	0.08	0.17	0.09
LN32D *vs* WT	VL	0.12	0.20	0.99	0.16	0.20
	VH	0.33	0.14	1.16	0.16	0.30
	HEL	0.59	0.87	0.16	0.74	0.39
LN92D *vs* WT	VL	0.10	0.13	0.67	0.11	0.13
	VH	0.18	0.12	0.80	0.13	0.21
	HEL	0.41	0.56	0.15	0.49	0.28

Figure 1

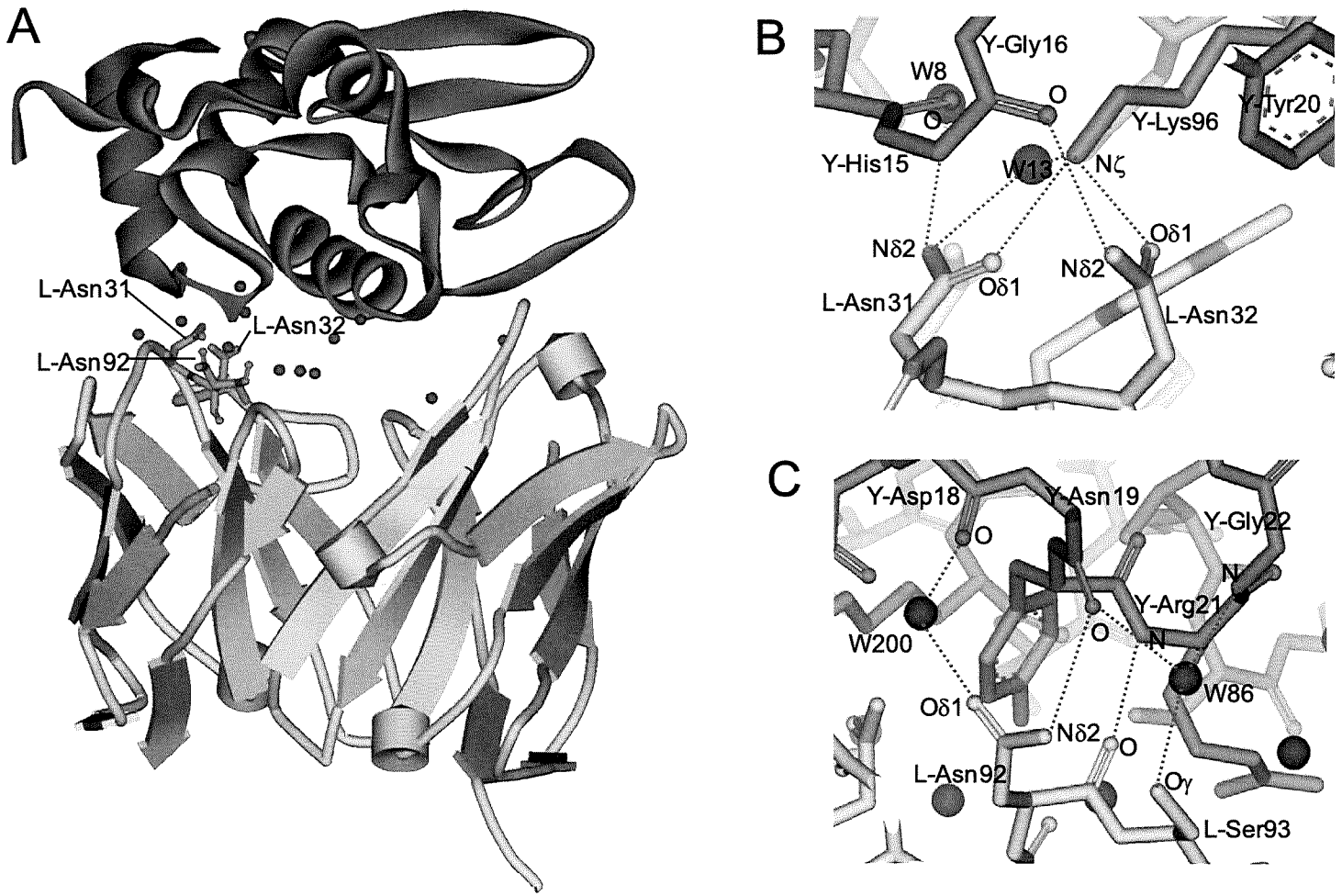

Figure 2

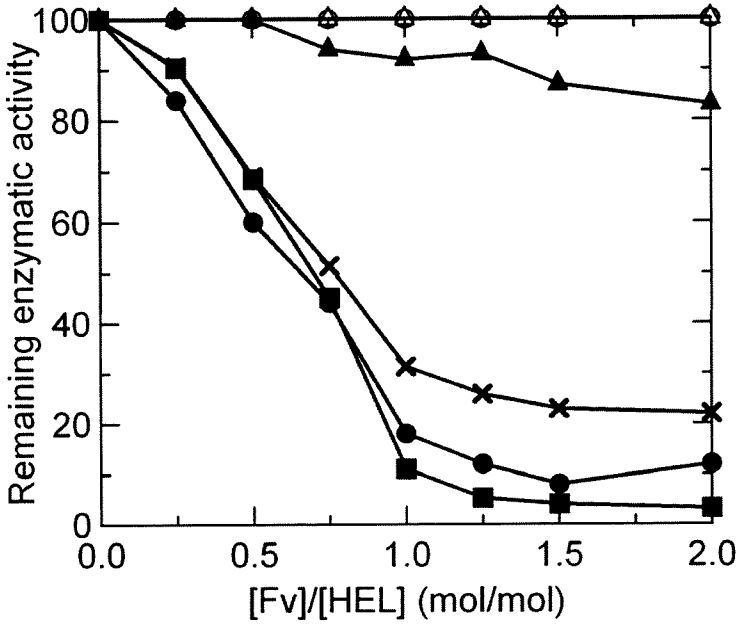

Figure 3

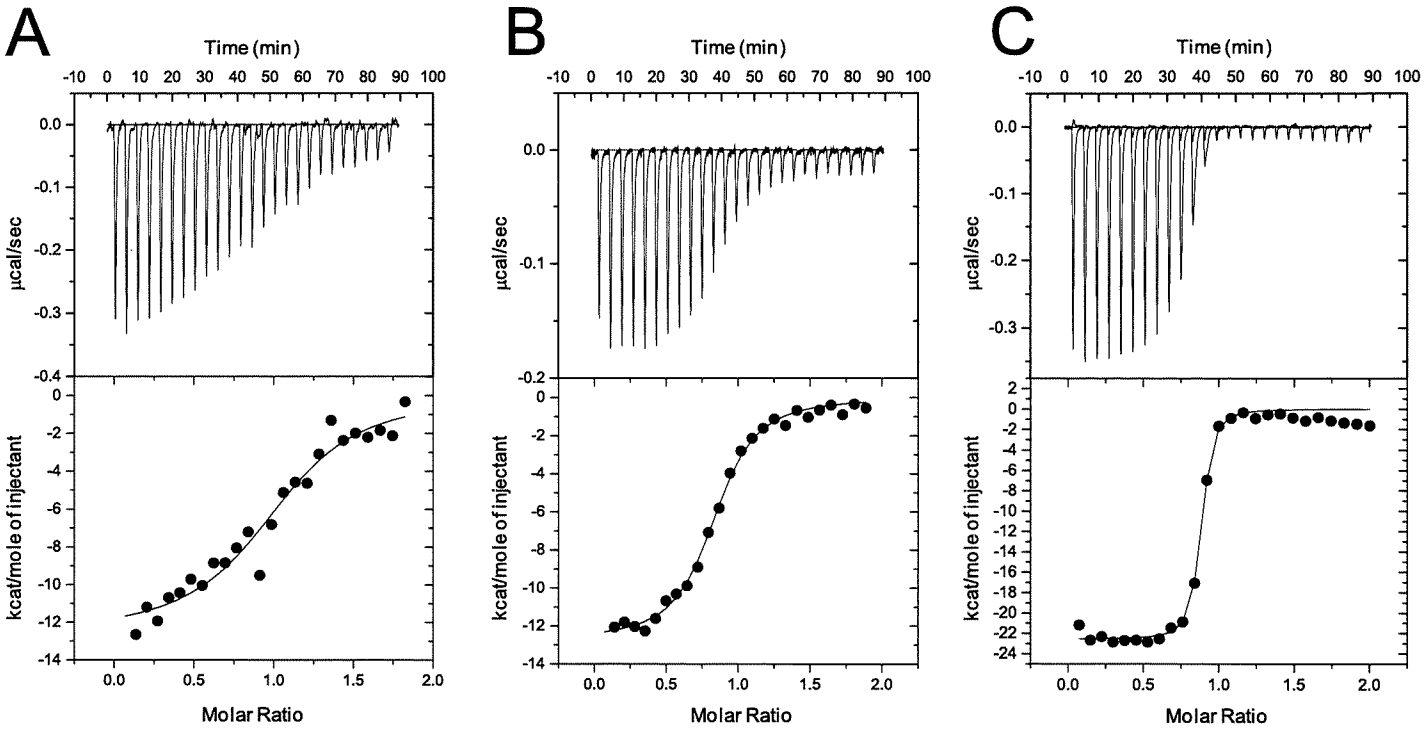

Figure 4

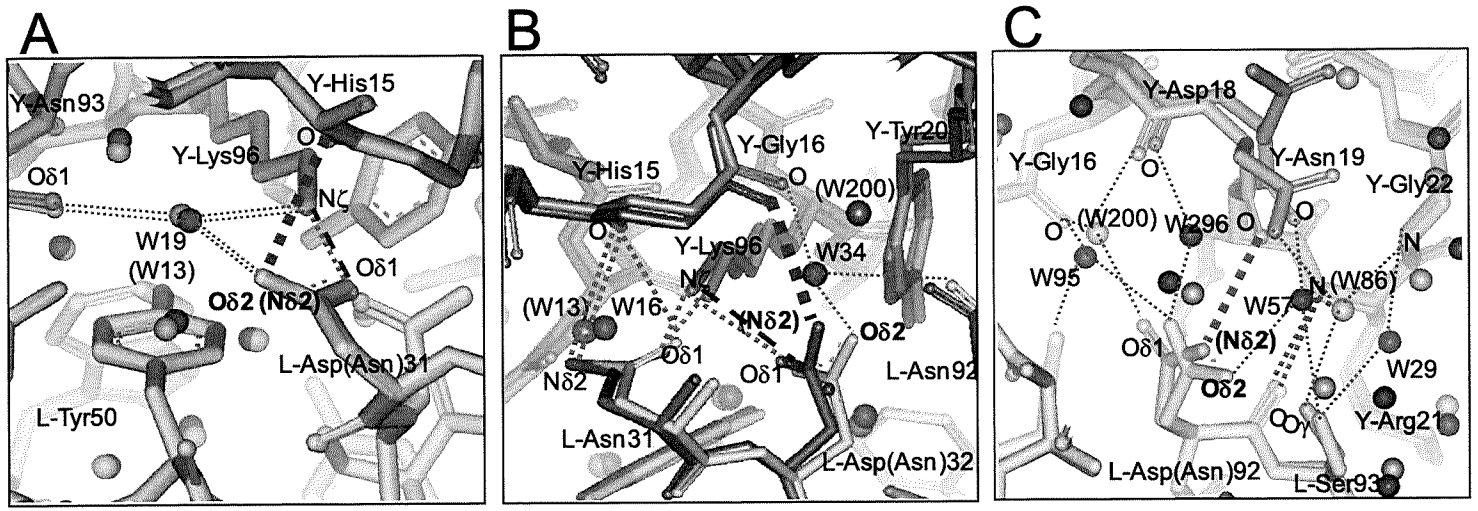

Figure 5

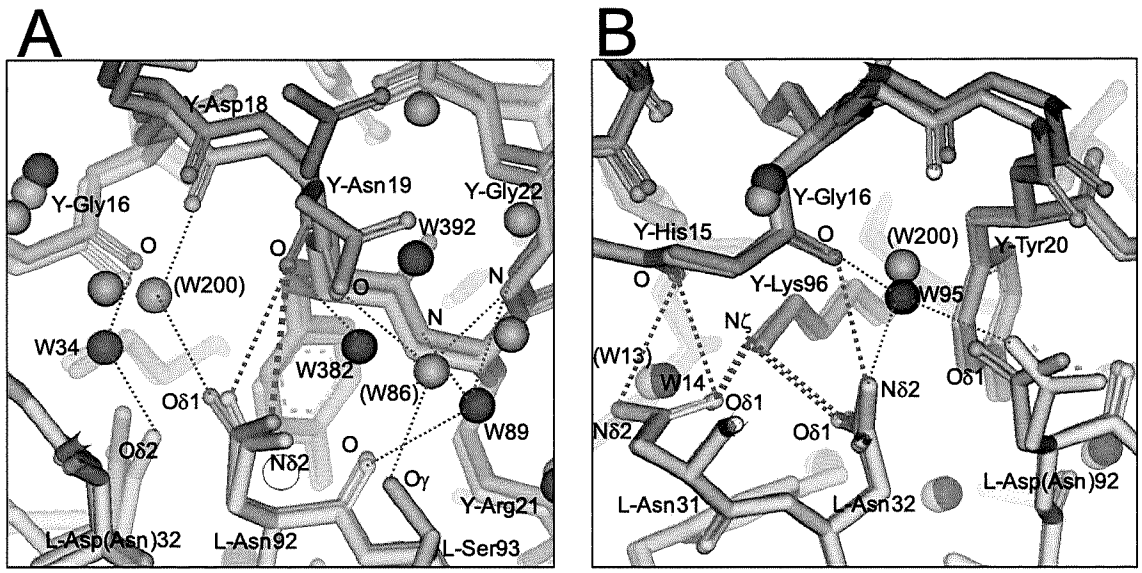

ARTICLE IN PRESS

JBIOSC-00316; No. of pages: 6; 4C:

Journal of Bioscience and Bioengineering
VOL. xx No. xx, xxx–xxx, 2009

ELSEVIER

www.elsevier.com/locate/jbiosc

Integration of PEGylation and refolding for renaturation of recombinant proteins from insoluble aggregates produced in bacteria—Application to a single-chain Fv fragment

Izumi Kumagai,* Ryutaro Asano, Takeshi Nakanishi, Kentaro Hashikami, Sho Tanaka, Adel Badran, Hideaki Sanada, and Mitsuo Umetsu

Department of Biomolecular Engineering, Graduate School of Engineering, Tohoku University, Aoba 6-6-11-607, Aramaki, Aoba-ku, Sendai 980-8579, Japan

Received 10 August 2009; accepted 16 October 2009

The conjugation of polyethylene glycol (PEGylation) with downsized compact antibodies is an effective method for overcoming the problem of rapid elimination of the compact antibodies from the body. We integrated site-specific PEGylation with the refolding of a single-chain Fv (scFv) of humanized monoclonal antibody 528 with affinity for the epidermal growth factor receptor, to prepare active PEGylated scFv from insoluble aggregates produced in an *Escherichia coli* expression system. The insertion of a cysteine residue at the C-terminus of scFv to serve as the conjugation site for PEG led to the formation of highly multimeric scFv during the refolding process; however, PEGylation after refolding drastically dispersed the multimer into monomeric active scFv fragments. Further, the PEGylation of partially refolded scFv during the refolding process improved the PEGylation efficiency and suppressed the formation of highly multimeric scFv; consequently, monomeric active scFv fragments were obtained directly from the insoluble aggregates in *E. coli*. We show that in vitro refolding of PEGylated scFv should be useful for improving downstream processing performance in the production of clinically useful small antibodies from insoluble fractions.

[**Key words:** In vitro refolding; PEGylation; Recombinant antibody; scFv; Therapeutic protein]

IgG-type antibodies are usually produced in mammalian cell expression systems, but the construction of a stable and large-scale production process in mammalian systems is laborious, time-consuming, and expensive. In contrast, antibody fragments, such as single-chain Fv (scFv) (1) and Fab fragments (2), can be prepared in bacterial secretory expression systems; however, the downsizing of antibodies has some benefits in protein expression processes, while it results in fast elimination of antibodies from the body to reduce medicinal benefits (3).

To overcome the problem of fast elimination, antibody fragments can be conjugated with polyethylene glycol (PEGylation) (4, 5). PEGylation of various therapeutic proteins has been widely studied as a means for improving pharmacokinetics and reducing immunogenicity (6, 7). The site-specific surface modification of anti-p185^{HER-2} antibody fragments by PEGylation is expected to improve pharmacokinetics and reduces immunogenicity without inactivating the fragments (8).

Another serious problem for compact antibodies is that secretory expression of the active antibody fragments in *Escherichia coli* is limited to the periplasm, because the reducing conditions in the cytoplasm prevent the formation of disulfide linkages, which are crucial for the immunoglobulin fold (9). In addition, some fragments form insoluble aggregates even in the periplasm (10, 11), and the fragments let us select an alternative approach of expression in the cytoplasm as inclusion bodies; consequently, refolding processes have been utilized for renaturing small molecular antibodies with scFv fragments, Fab fragments, and diabodies from their aggregated forms (9, 12-15). The refolding is generally accomplished by dilution of the denatured proteins in a refolding buffer. However, the dilution method does not always result in a high refolding yield, so a thiol–disulfide interchange reaction is used to increase the yield. The refolding efficiency can be improved by controlling the concentrations of thiol–disulfide exchange reagents and adding derivatives of solubilizing reagents, such as L-arginine (13, 14).

To prepare active PEGylated scFv from insoluble aggregates produced in *E. coli*, we integrated a site-specific PEGylation step with the refolding of the scFv fragment of a humanized monoclonal antibody 528 with affinity for the epidermal growth factor receptor (EGFR). PEGylation, besides clinical benefits, is expected to improve physicochemical properties of protein molecules (16): the high solubility of PEG molecules improves the solubility of PEGylated proteins, and the highly flexible polymer shields proteins against

Abbreviations: EDTA, ethylenediaminetetraacetic acid; EGFR, epidermal growth factor receptor; Fab, antigen binding fragment; Fv, variable fragment; mPEG, maleimide-PEG; scFv, single-chain Fv; Mw, molecular weight; PEG, polyethylene glycol; SDS-PAGE, sodium dodecyl sulfate-polyacrylamide gel electrophoresis; VH, heavy chain in Fv; VL, light chain in Fv; YT, yeast triptone.

* Corresponding author. Tel.: +81 22 795 7274; fax: +81 22 795 6164.
E-mail address: kmiz@kuma.che.tohoku.ac.jp (I. Kumagai).

1389-1723/$ - see front matter © 2009, The Society for Biotechnology, Japan. All rights reserved.
doi:10.1016/j.jbiosc.2009.10.016

Please cite this article as: Kumagai, I., et al., Integration of PEGylation and refolding for renaturation of recombinant proteins from insoluble aggregates produced in bacteria—Application to a single-chain Fv fragment, J. Biosci. Bioeng. (2009), doi:10.1016/j.jbiosc.2009.10.016

protease (17), immune system (17), irreversible aggregation (18), and so on. The integration resulted in the production of monodispersed active scFv fragments from insoluble aggregates in *E. coli*, and highly efficient refolding of monomeric PEGylated scFv fragments was accomplished. We show that in vitro refolding of PEGylated scFv fragments could improve downstream processing performance in the production of clinically useful small antibodies from insoluble fractions.

MATERIALS AND METHODS

Construction of expression vector To accomplish site-specific PEGylation of scFv, we used the method reported by Kubetzko et al. (8). We constructed an expression plasmid for humanized 528 scFv (h528 scFv) of VL-VH with a pelB leader sequence at the N-terminus of VL domain and a cysteine residue fused at the C-terminus of the VH domain by way of a c-*myc* tag, poly-histidine tag ($(His)_6$), and two glycine residues (h528 scFv-cys). The cysteine residue was introduced by polymerase chain reaction using the primers NcoI-h5H (5′-NNNNCCATGGCCCAGGTGCAACTGGTT-CAGAGCG-3′) and His-tag-Gly2-Cys (5′-ACTAGTCTAACATCCCCCGTGGTGGTGAT-GATGGTGCGA-3′), and the amplified sequences of h528 scFv-cys were inserted into pRA vectors.

Preparation, solubilization, and purification of denatured h528 scFv-cys Transformed *E. coli* BL21 (DE3) cells were incubated in 2×YT medium at 28 °C, and the expression of h528 scFv-cys under the control of the T7 promoter was induced by the addition of 1 mM isopropyl β-D-thiogalactopyranoside. The harvested cells were centrifuged and suspended in PBS buffer. After sonication, the suspension was centrifuged at 5800×*g* for 30 min at 4 °C. The pellet was solubilized in PBS buffer with 6 M guanidine HCl (GdnHCl), and then the supernatant was purified by means of a metal-chelate chromatography column that interacted with the poly-histidine tag in scFv; the adsorbed scFv-cys in the column was eluted with 50 mM imidazole in PBS with 6 M GdnHCl.

Renaturation of solubilized h528 scFv-cys The concentration of solubilized and purified scFv-cys was adjusted to 7.5 μM in a PBS solution containing 6 M GdnHCl. The scFv-cys solution (10 ml) was dialyzed against 500 ml of a PBS solution containing 0.4 M L-arginine and then against 500 ml of an L-arginine-free PBS solution to remove the denaturant and the stabilizing reagent. Each dialysis was performed for 12 h at 4 °C. For denaturation and renaturation processes of scFv from insoluble fraction, no redox reagents were used, because scFv with pelB sequence can be renatured from insoluble aggregates without redox reagents (19, 20) and h528 scFv has been efficiently renatured without redox reagents (15).

Pegylation of h528 scFv-cys The PEGylation was carried out either on the refolded scFv (after the final dialysis) or on the partially refolded scFv (before the removal of L-arginine). In the first case (Scheme I in Fig. 1), the C-terminal cysteine residue of h528 scFv-cys was activated by incubation for 30 min at 37 °C with 3 mM dithiothreitol after the removal of L-arginine. The activated h528 scFv-cys was loaded on a gel filtration column (HiPrep 26/10 desalting column; GE Healthcare Bio-Science, Piscataway, NJ, USA) to remove the reducing reagent and to exchange PBS for a citric acid solution (100 mM citric acid, 100 mM ammonium acetate, 2 mM EDTA, pH 6.0). The resulting proteins were incubated with a 10-fold molar excess of maleimide-PEG5 (MW, 5522 Da; NOF, Japan) or maleimide-PEG20 (MW, 20.858 kDa; NOF, Japan) for 2 h at 37 °C, and the PEGylated h528 scFv-cys was fractionated by gel filtration chromatography (Hiload Superdex 200-pg column 10/300; GE Healthcare Bio-Science).

In the second case (Scheme II in Fig. 1), the C-terminal cysteine residue of h528 scFv-cys was activated before the removal of L-arginine. The buffer exchange and PEGylation were performed in the presence of L-arginine, and L-arginine was removed after PEGylation.

Sodium dodecyl sulfate–polyacrylamide gel electrophoresis (SDS-PAGE) All the proteins in the supernatant were precipitated with 6% trichloroacetic acid and 0.083% sodium deoxycholate. The pellets were solubilized in a 1.4% SDS solution (3.8 mM Tris-HCl, 10% bromophenol blue, 6% glycerol) and then loaded onto an SDS-polyacrylamide gel sheet (12.5% acrylamide) using the buffer system described by Laemmli (21). For the analysis under reducing condition, 5% 2-mercaptoethanol was added in the 1.4% SDS solution.

Flow cytometry assay of the antigen binding activity of refolded 528 scFv The PEGylated scFv was purified with a gel filtration chromatography column of Hiload Superdex 200-pg (10/300; GE Healthcare Bio-Science, Piscataway, NJ), and test A431 cells of a human epidermoid cancer cell line (1×10^6) were incubated on ice with 200 pmol of purified PEGylated scFv for 30 min. The added incubated cells were washed with a PBS solution containing 0.1% NaN_3 and then exposed for 30 min on ice to fluorescein isothiocyanate-conjugated secondary antibody with affinity for the c-*myc* tag (9E10, Santa Cruz Biotechnology, Santa Cruz, CA, USA). The stained cells were analyzed by flow cytometry (FACSCalibur, Becton Dickinson, San Jose, CA, USA) (22).

RESULTS

Expression and refolding of 528 scFv-cys FRAGMENT For site-specific PEGylation at the C-terminus of the VH domain, we constructed an h528 scFv-cys fragment with a cysteine residue at the C-terminus of VH. In the *E. coli* expression system, h528 scFv-cys was expressed as insoluble material with few intermolecular disulfide linkages between expressed h528 scFv-cys fragments (Fig. 2).

To prepare soluble h528 scFv-cys, we solubilized the insoluble materials in 6 M GdnHCl solution, and then the solubilized h528 scFv-cys was refolded by means of dialysis against a denaturant-free solution via a 0.4 M L-arginine solution. Only a small amount of insoluble h528 scFv-cys aggregates formed during the refolding process; the yield of soluble protein was 88% of the solubilized protein.

Pegylation of h528 scFv-cys For PEGylation of the scFv-cys fragment, we reacted mPEG-5 or mPEG-20 with the refolded h528 scFv-cys fragment (Scheme I in Fig. 1) or with the partially refolded intermediate (Scheme II in Fig. 1). For the PEGylation of the partially refolded intermediate, mPEG was allowed to react with the partially refolded scFv-cys at the refolding stage in a 0.4 M L-arginine solution. Fig. 3 shows the SDS-PAGE and Western blotting results for h528 scFv-cys after PEGylation. When the PEGylation reaction was carried

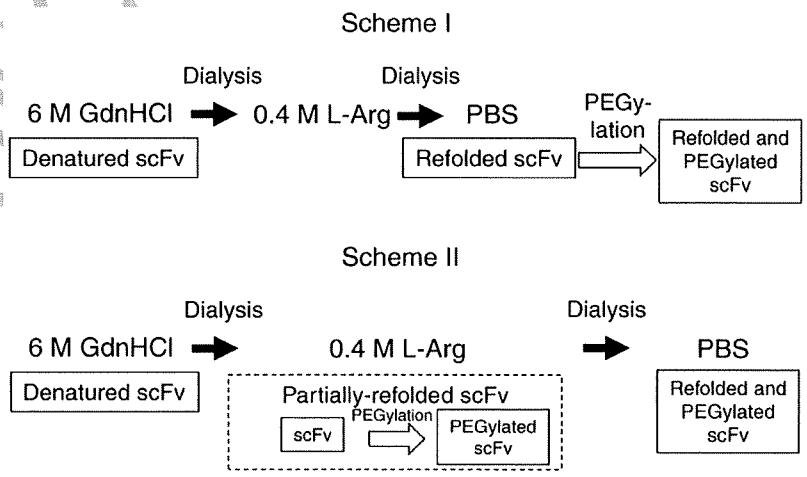

FIG. 1. Schemes for the integration of PEGylation with the stepwise refolding of scFv-cys. Scheme I: scFv-cys is PEGylated after the refolding process; Scheme II: scFv is PEGylated during the refolding process.

Please cite this article as: Kumagai, I., et al., Integration of PEGylation and refolding for renaturation of recombinant proteins from insoluble aggregates produced in bacteria—Application to a single-chain Fv fragment, J. Biosci. Bioeng. (2009), doi:10.1016/j.jbiosc.2009.10.016

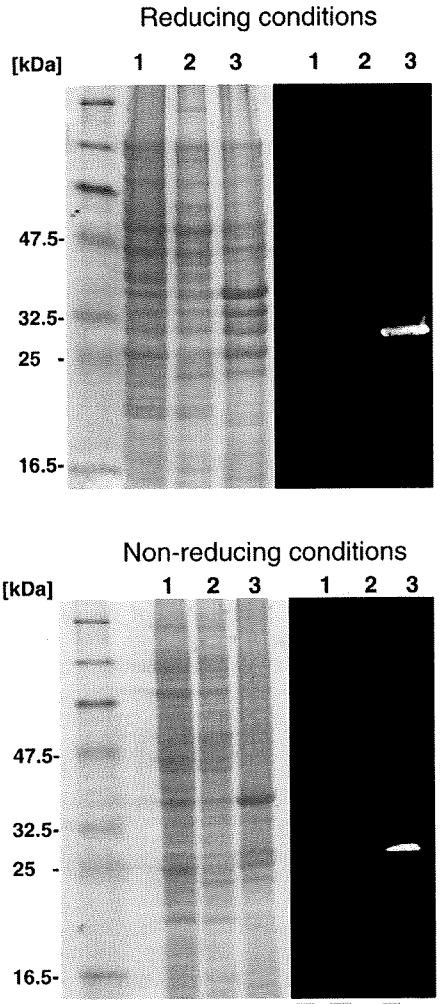

FIG. 2. (Left) SDS–PAGE and (right) Western blotting results for the h528 scFv-cys fragments expressed in an *E. coli* system under reducing and nonreducing conditions: media fraction (lane 1), soluble fraction (lane 2), and insoluble fraction (lane 3). In Western blotting, the protein band corresponding to h528 scFv-cys was detected using anti-His-tag antibody.

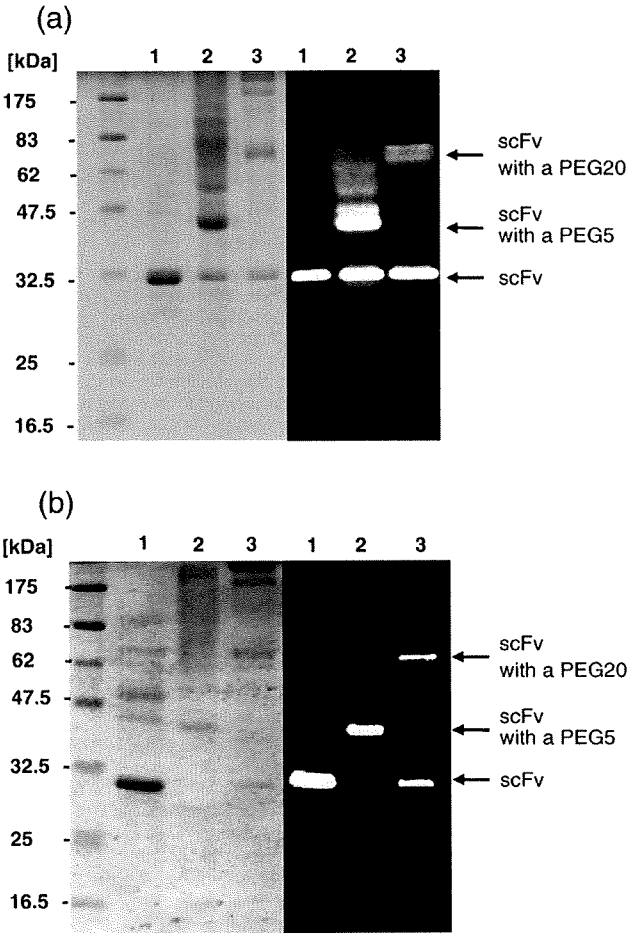

FIG. 3. (Left) SDS–PAGE and (right) Western blotting results for (a) h528 scFv-cys PEGylated (a) after refolding and (b) during refolding: untreated scFv-cys (lane 1), scFv-cys PEGylated with mPEG-5 (lane 2), and scFv-cys PEGylated with mPEG-20 (lane 3). In Western blotting, the protein band corresponding to h528 scFv-cys was detected using anti-His-tag antibody.

out with mPEG-5 after refolding, more than half of the scFv-cys fragments showed increased molecular weights (Fig. 3a); the strongest band corresponded to scFv-cys conjugated with one mPEG-5 molecule. The use of mPEG-20 also afforded scFv conjugated with one mPEG-20 molecule, but the increase in the molecular weight of the PEG molecule from 5 kDa to 20 kDa decreased the chemical conjugation efficiency. This result indicates that the size of the PEG molecule affected the conjugation reaction with refolded h528 scFv-cys.

As was the case for PEGylation after refolding, PEGylation of the partially refolded scFv-cys in a 0.4 M L-arginine solution predominantly afforded scFv conjugated with one PEG molecule (Fig. 3b); however, the SDS–PAGE and Western blotting results for PEGylation with mPEG-5 showed little unreacted scFv. This result indicates that the conjugation efficiency for the PEGylation of the partially refolded scFv-cys is higher than that of the refolded scFv-cys.

Analysis of size distribution by gel filtration chromatography We examined the gel filtration chromatographies of scFv-cys PEGylated with mPEG-5 (Fig. 4). Before PEGylation, only a small amount of the refolded scFv-cys existed in monomeric form (solid arrow in Fig. 4a); the majority of the scFv-cys existed in highly multimeric forms (broken arrow in Fig. 4a). In contrast, PEGylation of the multimeric scFv-cys (Scheme I) led to a drastic transformation to a monomeric scFv-cys form (Fig. 4b). Analysis of the molecular weight distribution by means of SDS–PAGE indicated that the monomeric form was scFv-cys conjugated with one mPEG-5 molecule, whereas the residual multimeric forms consisted only of unreacted scFv-cys (data not shown). This result indicates that monomeric PEGylated scFv was generated from soluble aggregates formed during the refolding process.

When PEGylation was carried out during the refolding process (Scheme II), monomeric scFv-cys fragments conjugated with one mPEG-5 molecule were also obtained (Fig. 4c), and this result was confirmed by SDS–PAGE. The gel filtration chromatography results for the partially refolded scFv-cys intermediate in the 0.4 M L-arginine stage showed that the intermediate was eluted in 14–15 ml fractions (Fig. 4d), which corresponded to be a monomeric form when we made a calibration curve of used column for molecular weight using the 0.4 M L-arginine refolding solution. This result indicates that PEGylation suppressed the aggregation of the partially refolded scFv-cys intermediate during the refolding process.

Please cite this article as: Kumagai, I., et al., Integration of PEGylation and refolding for renaturation of recombinant proteins from insoluble aggregates produced in bacteria—Application to a single-chain Fv fragment, J. Biosci. Bioeng. (2009), doi:10.1016/j.jbiosc.2009.10.016